Bioresource Technology 216 (2016) 150–158

Contents lists available at ScienceDirect

Bioresource Technology

journal homepage: www.elsevier.com/locate/biortech

Temperature regulates methane production through the function centralization of microbial community in anaerobic digestion

Qiang Lin [a,b], Jo De Vrieze [c], Guihua He [a], Xiangzhen Li [a], Jiabao Li [a,*]

[a] Key Laboratory of Environmental and Applied Microbiology, CAS, Environmental Microbiology Key Laboratory of Sichuan Province, Chengdu Institute of Biology, Chinese Academy of Sciences, Chengdu 610041, China
[b] University of Chinese Academy of Sciences, Beijing 100049, China
[c] Laboratory of Microbial Ecology and Technology, Ghent University, Coupure Links 653, B-9000 Gent, Belgium

HIGHLIGHTS

- Temperature-regulated mechanism in AD process is revealed by metatranscriptome.
- Methanogenesis and oxidative phosphorylation are enhanced at elevated temperature.
- Function centralization is crucial for the efficiency of AD system function.
- Temperature regulates AD process by the centralization of functional pathways.

ARTICLE INFO

Article history:
Received 4 April 2016
Received in revised form 12 May 2016
Accepted 14 May 2016
Available online 18 May 2016

Keywords:
Anaerobic digestion
Temperature
Functional diversity
Function centralization
Metatranscriptome

ABSTRACT

Temperature is crucial for the performance of anaerobic digestion process. In this study of anaerobic digestion of swine manure, the relationship between the microbial gene expression and methane production at different temperatures (25–55 °C) was revealed through metatranscriptomic analysis. Daily methane production and total biogas production increased with temperature up to 50 °C, but decreased at 55 °C. The functional gene expression showed great variation at different temperatures. The function centralization (opposite to alpha-diversity), assessed by the least proportions of functional pathways contributing for at least 50% of total reads positively correlated to methane production. Temperature regulated methane production probably through reducing the diversity of functional pathways, but enhancing central functional pathways, so that most of cellular activities and resource were invested in methanogenesis and related pathways, enhancing the efficiency of conversion of substrates to methane. This research demonstrated the importance of function centralization for efficient system functioning.

1. Introduction

Temperature is one of most important factors that affect stability and performance of anaerobic digestion (AD) process (De Vrieze et al., 2015; Pap et al., 2015). In AD systems, thermodynamic equilibrium of the biochemical reactions (Wilson et al., 2008) and microbial community structure, activities and diversity (Gannoun et al., 2016; Gunnigle et al., 2015; Sun et al., 2015) can be influenced by temperature. For example, methanogens show higher growth rates at thermophilic condition, which may induce efficient methane production (Sun et al., 2015; Weiland, 2010). An increase of hydrogenotrophic methanogens at 55 °C compared to 35 °C (Tian et al., 2015), may result in alternative methanogenic pathways in AD (Li et al., 2014; Pap et al., 2015). However, most of these studies focus on microbial community composition, but rarely on metabolic activities inferred from microbial community gene expression. Microbial community gene expression, in contrast to microbial community composition, associates more tightly with system functioning (de Menezes et al., 2012; Shi et al., 2014). The gene expression based Metatranscriptomic analysis, which refers to active metabolic pathways or microorganisms, more actually reflects immediate changes in metabolic profiles corresponding to *in situ* system performance (Vanwonterghem et al., 2014). In sheep rumen microbiome, for example, the expression of methanogenesis pathway based on Metatranscriptomic analysis shows a positive correlation with methane production, whereas such a pattern cannot be shown based on metagenomics analysis (Shi et al., 2014). However, the mechanism of temperature

* Corresponding author.
E-mail address: Lijb@cib.ac.cn (J. Li).

http://dx.doi.org/10.1016/j.biortech.2016.05.046
0960-8524/

effects on the microbial community gene expression to regulate methane production in AD systems has been rarely reported.

The relationship between the microbial community diversity and system functioning has been investigated comprehensively (Fredriksson et al., 2012; Wittebolle et al., 2009). The initial evenness of the microbial community is considered as one of the most important factors to guarantee functional stability (Wittebolle et al., 2009), which is supported further by the fact that a higher degree of functional stability is tightly related with the evenness of a bacterial community in AD systems (De Vrieze et al., 2013). Especially, a high microbial community evenness has been shown to improve methane production (Werner et al., 2011), likely due to the fact that high diversity provides more functional redundancy (Naeem and Li, 1997). However, some specific microorganisms, such as *Clostridium* species, are involved in multiple steps of anaerobic digestion, and some specific steps are shared by various microorganisms (Vanwonterghem et al., 2014), thus the diversity of the microbial community cannot reflect the actual diversity of system functioning.

The diversity of system functioning in AD systems is crucial for oriented and efficient conversion of organic waste to methane, because methane is not the only metabolite in AD process (Weiland, 2010). Compared to the diversity of a microbial community, the diversity of functional pathways can more synchronously and authentically reflect the diversity of system functioning. However, few researches have evaluated the relationship between the diversity of functional pathways (and even the centralization of functional pathways) and the efficiency of specific system functioning, such as methane production in AD systems. Hence, whether diversity of functional pathways shares similar mechanisms with the diversity of a microbial community to regulate system functioning needs further investigation.

In this study, the variation of functional pathways at different temperatures from 25 to 55 °C, were investigated based on Metatranscriptomic analysis, to reveal the temperature-regulated microbial effects on system functioning in AD process. We evaluated (i) the variation of functional pathways under a temperature gradient, (ii) the relationship between the variation of functional pathways and methane production, and (iii) whether the diversity of functional pathways shares similar mechanisms with microbial community diversity with respect to methane production.

2. Materials and methods

2.1. Experimental set-up

The anaerobic digestion experiment was performed with 1.5 L of digestion sludge, with a total solids (TS) content of 8% in a 2 L anaerobic flask with two holes on the upper and lower flask-wall (Supplementary Table S1). Feeding and digestate removal through the upper and lower hole, respectively, was carried out by a peristaltic pump (Cat. No. BT50 s, Leadfluid, China). At the start of the experiment, 450 mL seed sludge was inoculated. Seed sludge was prepared by semi-continuous AD of swine manure (obtained from a pig farm in Chengdu, Sichuan Province, China) under the respective experimental temperature at a hydraulic retention time (HRT) of 30 days, for at least two times the HRT, until the digestion performance was maintained at a dynamic equilibrium, with biogas containing more than 60% of CH_4. The different treatments were set up at 25, 35, 50 and 55 °C, with triplicate incubations for each temperature. Swine manure was used as substrate. After daily CH_4 production reached a first peak in the reactor, a semi-continuous feeding mode was implemented in which 150 mL of digestate was replaced with the same volume of fresh swine manure slurry every three days. The organic loading rate (OLR) was set at 2.0 g volatile solids (VS) L^{-1} day^{-1} to ensure that a dynamic equilibrium (stable period) could be maintained during the fermentation process. The reactor was shaken manually twice a day to mix the digestion sludge. The detailed parameters at the start of the experiment were shown in Supplementary Table S1.

2.2. Sampling and chemical analysis

The sludge samples were collected in the initial period (24 h after digestion start, only used for chemical analysis) and the stable period (48 h after the second feed, used for both chemical and microbial community analysis) (Supplementary Table S2). The sludge in the stable period was pelleted by centrifugation at 13,400*g* for 10 min at 4 °C, and immediately used for RNA extraction. The supernatant was filtered through a 0.22 μm filter (Cat. No. SLGP033RS; Millipore, USA). Nessler's reagent colorimetric method was used to quantify NH_4^+–N concentration (Hart et al., 1994). The volatile fatty acids (VFAs) in the supernatant were detected by Agilent 1260 Infinity liquid chromatography (Agilent Technologies, USA), equipped with a column Hi-Plex H (300 × 6.5 mm) and a differential refraction detector. The mobile phase was H_2SO_4 (0.005 M) with a flow rate of 0.6 mL min^{-1}. TS, VS and chemical oxygen demand (COD) were measured as previously described (APHA, 1998). The volume of biogas production was measured by water replacement method. The water replacement equipment was set at air pressure (about 95.86 kpa) and room temperature (about 22 °C), which avoided the bias of the measured volume caused by different pressures and temperatures. Then, the volume of the gas was normalized at standard temperature (273 K) and pressure (101325 Pa), based on the ideal gas law (Bludman and Vanriper, 1977). The CH_4 and H_2 content of the biogas were measured with an Agilent 6890 gas chromatography system (Agilent Technologies, USA), equipped with a 2 m stainless steel column packed with Porapak Q (50/80 mesh) and with a thermal conductivity detector. The injection port, column oven, and detector were operated at 100, 70, and 150 °C, respectively. The carrier gas was argon with a flow rate of 30 mL min^{-1}. Standard gases (72.15% CH_4, 3.49% H_2 and 24.36% CO_2) (Hongjin, China) were used for calibration before each measurement.

2.3. RNA extraction and Metatranscriptomic sequencing

Total RNA was extracted using the RNAprep pure Cell/Bacteria Kit (Cat. No. DP430; TIANGEN, China). Ribosomal RNA was removed from the total RNA using the RiboMinusTM kit (Lot. No. 1539791; Invitrogen, USA). The Metatranscriptomic sequencing was performed using an Illumina Hiseq 2000 (Illumina Inc., USA). The obtained sequences from total 12 samples were uploaded to MG-RAST (Meyer et al., 2008) under the project "zf-temperature-underreplication" with assigned MG-RAST ID (4606650.3, 4606661.3, 4606660.3, 4606659.3, 4606658.3, 4606657.3, 4606656.3, 4606655.3, 4606654.3, 4606653.3, 4606652.3 and 4606651.3) for further analysis. Before the Metatranscriptomic analysis, poor quality sequences were removed through the MG-RAST version 3.6 online server quality control pipeline (Meyer et al., 2008). The average uploaded sequences in each sample were 21,860,657 ± 2,077,558, of which around 57% could be annotated as predicted protein. Finally, identified functional categories in each sample were on average 119,462 ± 23,938. The annotation of phylogenetically defined microorganisms was based on the KEGG database. The annotation of functional profiles was based on the KEGG Orthologs (KO) database in which the all annotation levels were considered for a comprehensive evaluation. The functional annotation consisted of four levels. The highest level in the KEGG categories was presented as level 1, followed by level 2. Level 3 reflected the KEGG pathways, and level 4 (gene expression

level) contained expression of specific genes with entail enzyme commission (EC) numbers (Millares et al., 2015; Yu and Zhang, 2012). The other pipeline parameters were kept at default settings, minimum alignment length of 15, maximum e-value of 10^{-5} and minimum identity of 60%. The microorganisms mainly involved in functional pathways were detected through the pipeline of workbench. The reads of taxonomic and functional profiles at different hierarchical levels were normalized using daisychopper.pl (http://www.festinalente.me/bioinf/downloads/daisychopper.pl), respectively, to calculate the relative abundances of specific functional taxa, based on total reads.

2.4. Statistical analysis

The general changes of the functional profiles at the different temperatures were assessed by Permutational multivariate analysis of variance (PERMANOVA) and principal coordinates analysis (PCoA) based on the Bray-Curtis dissimilarity index performed using the ape package in R (http://www.r-project.org/). The normality and homoscedasticity of the raw data were validated by means of the SPSS 21 software (IBM USA). One-way-analysis of variance (ANOVA) performed in SPSS 21 was used to test the differences in relative abundances of functional units between samples at different temperatures. Pearson's and Spearman's correlation analysis, alpha-diversity indices (Shannon index, Pielou's evenness and Simpson' diversity index) and redundancy analysis (RDA) were calculated in R with the vegan package. The Gini coefficient was calculated as previously described (Marzorati et al., 2008).

3. Results and discussion

3.1. Digester performance

Each treatment was inoculated with 30% of seed sludge. After daily CH_4 production (DCP) reached the first peak, the dynamic equilibrium was observed until the end of fermentation (Fig. S1). The DCPs in stable period reached 0.34 ± 0.03, 0.63 ± 0.01, 1.44 ± 0.09 and 0.81 ± 0.08 L L^{-1} day^{-1} at 25, 35, 50 and 55 °C, respectively. Total biogas production over 27 days reached 555.6 ± 14.1 L kg^{-1} VS at 50 °C, followed by 277.1 ± 27.4 L kg^{-1} VS at 55 °C (Fig. S1). The CH_4 content in the biogas remained constant during the stable period, and was higher at 50 and 55 °C (around 60%), compared to 25 and 35 °C (Fig. S2). The H_2 content in the biogas remained between 0.1% and 0.8% during the entire experiment. Due to a similar pattern of the DCP and total biogas production at each temperature, the DCP was used to represent methane production in the following analyses.

3.2. VFAs dynamics

Acetic acid, propionic acid and butyric acid were main VFAs, and they varied dramatically along the temperature gradient (Fig. S3), indicating different fermentation conditions. At temperatures from 35 to 55 °C, the concentrations of acetic acid decreased over time, reaching 2–4 mM, in the stable period. The concentrations of propionic acid and butyric acid showed the similar trend as acetic acid. However, at 25 °C, propionic acid and butyric acid accumulated up to about 22 mM and 37 mM, respectively, in the stable period. During the fermentation process from initial period to stable period, the highest VFAs conversion rates were detected at 50 °C, and the lowest at 25 °C.

The concentrations of NH_4^+–N remained at 320–780 mg L^{-1} in the stable period (data not shown). The initial pH value was 7.0, and it gradually increased to 7.4–7.8 until the stable period at each temperature.

3.3. Functional profiles

PCoA and PERMANOVA tests showed a significant variation ($p < 0.001$) at level 4 (gene expression level) at different temperatures (Supplementary Fig. S4). This indicated that temperature played a crucial role in the global regulation of gene expression. Further analysis of functional category at KEGG level 1 (Supplementary Fig. S5) showed that the category "metabolism" had the highest relative abundance, with more than 50% of total reads at each temperature, and positively correlated with DCP ($p < 0.05$). At KEGG level 2 (Fig. 1), the samples at 25 and 35 °C clustered more closely, and the samples at 50 and 55 °C clustered closely, indicating the overall differences in microbial functional profiles between mesophilic (25–35 °C) and thermophilic (50–55 °C) conditions. Among different functional groups, amino acid metabolism, nucleotide metabolism and lipid metabolism showed significant negative correlations with temperature ($p < 0.01$). In contrast, both membrane transport and cell motility showed a positive correlation with temperature ($p < 0.01$). The category "energy metabolism", with highest relative abundance, significantly and positively correlated with DCP ($p < 0.01$). At KEGG level 3, among the functional pathways that were affiliated to energy metabolism, methane metabolism (ko00680, mainly referred to methanogenesis in anaerobic environments) and oxidative phosphorylation (ko00190) were dominant at all temperatures (Fig. 2). Redundancy analysis showed that inside the energy metabolism, only methane metabolism and oxidative phosphorylation positively contributed to methane production (Supplementary Fig. S6), but they showed no significant correlation with temperature, indicating that both methane metabolism and oxidative phosphorylation played important roles in methane production at all temperatures.

At KEGG level 3, in total 105 functional pathways were shared at all temperatures, occupying 79–94% of all pathways identified at level 3 (Supplementary Fig. S7). This indicated a high conservation of the expression ranges of functional pathways at different temperatures. At level 3, the pathway with the highest average relative abundance at all temperatures was methane metabolism, followed by ATP-binding cassette (ABC) transporters (ko02010), ribosome (ko03010), flagellar assembly (ko02040), and oxidative phosphorylation (ko00190) (Table 1). Among these abundant functional pathways, only methane metabolism and oxidative phosphorylation showed a significant positive correlation with DCP ($p < 0.01$). The main contributors to these pathways at different temperatures were further detected (Table 2). The phyla mainly involved in the pathway of ribosome were Firmicutes, Bacteroidetes and Euryarchaeota (nearly all of microorganisms in Euryarchaeota were identified as methanogens in this study) at mesophilic (25–35 °C) condition, but at thermophilic (50–55 °C) condition, Thermotogae took place of Bacteroidetes, indicating the different adaptive strategies of various microorganisms to temperature. The phyla mainly involved in the pathway of flagellar assembly at different temperatures also reflected similar adaptive strategies to temperature. Overall, the pathway of oxidative phosphorylation was mainly attributed by Euryarchaeota at different temperatures.

3.4. Conservation and variation of functions at different temperatures

In this study, a high conservation of expression range of functional pathways was observed under a temperature gradient, which might be the common responses of microbial community under anaerobic digestion. However, an obvious variation in relative abundance of functional pathways, which corresponded well with methane production, was detected at different temperatures. Especially at level 3, the relative abundances of methanogenesis could be regarded as an indicator of methane production in the

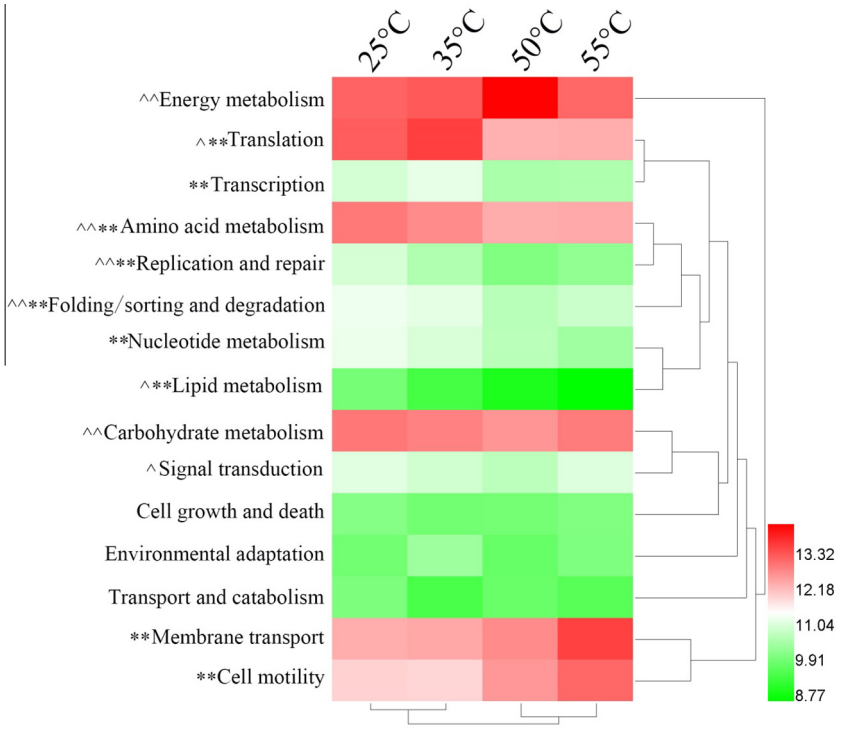

Fig. 1. Metabolic clustering at level 2, annotated based on KEGG Orthologs annotations at the different temperatures. A double hierarchical cluster is established through a weight-pair group clustering method, based on the Pearson distance. The heat map depicts the relative abundance of each category of pathways (variables clustering on the *y* axis) in each sample (*x* axis clustering). The color represents the normalized relative abundances of category of pathways in each sample. The pathways with relative abundance >1% are shown. **Significant correlation with temperature at $p < 0.01$; ^^significant correlation with DCP at $p < 0.01$, and ^at $p < 0.05$.

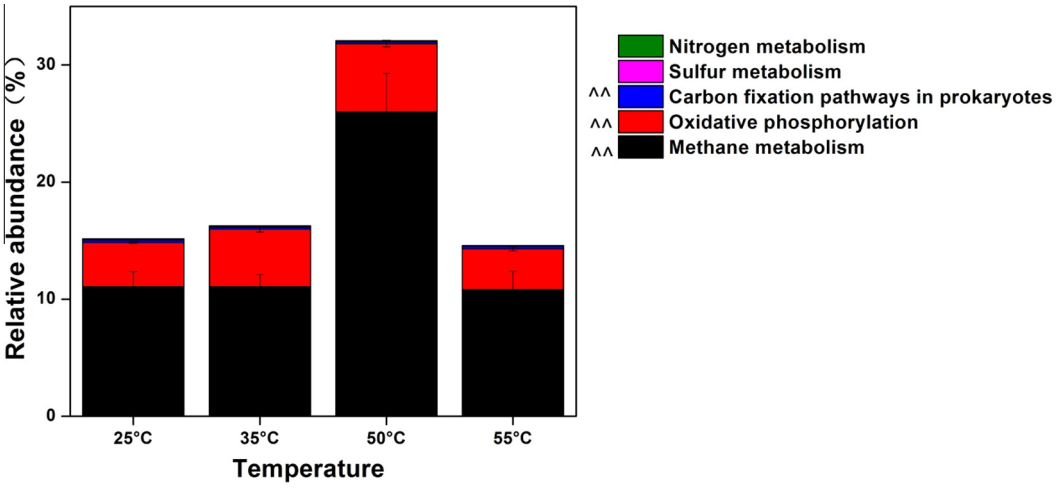

Fig. 2. Functional pathways at level 3, affiliated to energy metabolism at different temperatures. ^^Significant correlation with DCP at $p < 0.01$, ^at $p < 0.05$.

AD process, which agreed well with previous studies (Shi et al., 2014). The relative abundance of methanogenesis increased with temperature from 25 to 50 °C, most likely contributed by the higher growth rates of methanogens at thermophilic conditions (Weiland, 2010). Ribosomes that consist of ribosomal proteins based on the KO database play an important role in protein synthesis, and are regarded as indicators of growth rates (Gifford et al., 2013). Although the relative abundance of ribosomes negatively correlated with temperature, the contributive proportions of Euryarchaeota increased with temperature from 25 to 50 °C (Table 2), implicating that the growth of methanogens was elevated with temperature up to 50 °C. However, thermophilic digesters are more susceptible to inhibition (Labatut et al., 2014) and this study indicated that 50 °C might be the threshold temperature within which an increased temperature improves methane production in AD systems. In addition, this result was further supported by lower relative abundance of ribosomes and lower contributive proportions of Euryarchaeota in the relative abundances of this pathway at 55 °C compared to 50 °C.

Besides methanogenesis, the relative abundance of oxidative phosphorylation also showed a positive correlation with DCP ($p < 0.01$), probably because of the coupled relationship between oxidative phosphorylation and methanogenesis in the overall energy metabolism. Oxidative phosphorylation is responsible for energy conservation (Gifford et al., 2014), and in the methanogenesis electron transfer causes a proton gradient for ATP synthesis

Table 1
The functional pathways at level 3, annotated based on the KEGG Orthologs datasets at different temperatures. The taxa with average relative abundance >1% are shown.

Functional pathways at level 3	Temperature				Correlation				
	25 °C	35 °C	50 °C	55 °C	DCP	Temperature	Acetate	Propionate	Butyrate
Methane metabolism [PATH:ko00680]	11.06 ± 1.31b	11.06 ± 1.04b	25.98 ± 3.31a	10.81 ± 1.57b	.788**	.375	−.389	−.395	−.324
ATP-binding cassette (ABC) transporters [PATH:ko02010]	6.86 ± 0.21c	6.99 ± 0.36c	9.93 ± 0.56b	18.61 ± 0.62a	.221	.814**	−.442	−.730**	−.477
Ribosome [PATH:ko03010]	11.04 ± 0.9b	15.65 ± 0.22a	5.34 ± 0.18c	5.07 ± 0.08c	−.564	−.760**	.289	.627*	.284
Flagellar assembly [PATH:ko02040]	4.84 ± 0.6c	3.01 ± 0.17d	8.14 ± 0.92b	11.47 ± 0.09a	.411	.828**	−.398	−.709**	−.392
Oxidative phosphorylation [PATH:ko00190]	3.77 ± 0.08c	4.92 ± 0.24b	5.84 ± 0.29a	3.48 ± 0.19c	.708**	.148	−.466	−.228	−.419
Aminoacyl-tRNA biosynthesis [PATH:ko00970]	4.37 ± 0.43a	3.87 ± 0.05a	2.48 ± 0.13b	3.05 ± 0.1b	−.843**	−.826**	.757**	.847**	.695*
RNA polymerase [PATH:ko03020]	3.25 ± 0.06b	3.66 ± 0.03a	2.32 ± 0.1c	2.41 ± 0.04c	−.671*	−.815**	.428	.710**	.398
Bacterial chemotaxis [PATH:ko02030]	1.54 ± 0.06b	3.3 ± 0.24a	2.05 ± 0.16b	3.27 ± 0.56a	.056	.408	−.585*	−.470	−.626*
RNA degradation [PATH:ko03018]	3.07 ± 0.07a	2.8 ± 0.03a	1.78 ± 0.07c	2.3 ± 0.13b	−.913**	−.837**	.718**	.801**	.699*
Glycolysis/Gluconeogenesis [PATH:ko00010]	2.43 ± 0.06b	2.48 ± 0.03b	1.98 ± 0.15c	2.79 ± 0.06a	−.604*	.036	.073	−.012	.033
Glycine, serine and threonine metabolism [PATH:ko00260]	2.96 ± 0.09a	2.46 ± 0.07b	1.94 ± 0.14c	2.09 ± 0.08c	−.813**	−.891**	.861**	.919**	.840**
Purine metabolism [PATH:ko00230]	2.7 ± 0.14a	2.42 ± 0.03ab	2.09 ± 0.27bc	1.69 ± 0.06c	−.428	−.843**	.659*	.838**	.650*
Alanine, aspartate and glutamate metabolism [PATH:ko00250]	2.72 ± 0.18a	2.63 ± 0.17b	1.18 ± 0.07b	1.09 ± 0.01a	−.710**	−.934**	.668*	.894**	.633*
Pyruvate metabolism [PATH:ko00620]	1.54 ± 0.08b	2.13 ± 0.13a	1.52 ± 0.04b	2.07 ± 0.07a	−.186	.232	−.384	−.292	−.466
Plant-pathogen interaction [PATH:ko04626]	1.5 ± 0.06b	2.07 ± 0.08a	1.43 ± 0.14b	1.69 ± 0.03b	−.257	−.129	−.218	.022	−.288
Cell cycle - Caulobacter [PATH:ko04112]	1.68 ± 0.06	1.47 ± 0.05	1.51 ± 0.12	1.71 ± 0.13	−.217	.044	.365	.088	.279
HIF-1 signaling pathway [PATH:ko04066]	1.4 ± 0.13ab	1.46 ± 0.06ab	1.13 ± 0.09b	1.67 ± 0.16a	−.394	.088	−.008	−.073	−.019
Two-component system [PATH:ko02020]	1.56 ± 0.03a	1.12 ± 0.05b	1.34 ± 0.1ab	1.62 ± 0.21a	−.140	.131	.321	−.006	.310
Bacterial secretion system [PATH:ko03070]	1.58 ± 0.08a	1.73 ± 0.02a	1.01 ± 0.05b	1.17 ± 0.04b	−.736**	−.801**	.470	.734**	.437
Citrate cycle (TCA cycle) [PATH:ko00020]	1.33 ± 0.04a	1.25 ± 0.03a	0.96 ± 0.01b	1.25 ± 0.07a	−.877**	−.518	.593*	.541	.509
Peroxisome [PATH:ko04146]	1.47 ± 0.15a	0.85 ± 0.06c	1.28 ± 0.05ab	1.15 ± 0.03b	−.092	−.173	.484	.247	.582*
Cysteine and methionine metabolism [PATH:ko00270]	1.23 ± 0.17	0.9 ± 0.02	0.95 ± 0.07	1.21 ± 0.08	−.361	−.071	.502	.237	.425
Pentose and glucuronate interconversions [PATH:ko00040]	1.22 ± 0.08a	1.09 ± 0.02a	0.91 ± 0.03b	1.09 ± 0.05a	−.829**	−.596*	.616*	.657*	.652*
Pentose phosphate pathway [PATH:ko00030]	1.29 ± 0.06a	1.2 ± 0.07a	0.74 ± 0.08b	0.78 ± 0.02b	−.746**	−.907**	.705*	.861**	.671*

**Significantly at $p < 0.01$; *$p < 0.05$. All data are presented as means ± standard deviations. Values in a row with different letters mean significant differences at $p < 0.05$.

Table 2
Main microbial populations at phylum level participating in core functional pathways annotated based on the KEGG Orthologs datasets at different temperatures.

	25 °C	35 °C	50 °C	55 °C
Ribosome [PATH:ko03010]	Euryarchaeota (7.24 ± 1.51c) Bacteroidetes (22.33 ± 2.53b) Firmicutes (32.59 ± 1.89a)	Euryarchaeota (9.78 ± 0.17c) Bacteroidetes (19.21 ± 1.34b) Firmicutes (38.98 ± 2.79a)	Thermotogae (11.02 ± 1.5c) Euryarchaeota* (20.89 ± 1.12b) Firmicutes (52 ± 1.49a)	Euryarchaeota (14.84 ± 3.06c) Thermotogae (22.09 ± 3.72b) Firmicutes (51.02 ± 2.67a)
ATP-binding cassette (ABC) transporters [PATH:ko02010]	Actinobacteria (6.63 ± 0.6c) Proteobacteria (13.79 ± 0.07b) Firmicutes (48.2 ± 1.92a)	Actinobacteria (13.68 ± 3.04b) Proteobacteria (14.94 ± 2.08b) Firmicutes (43.35 ± 5.45a)	Euryarchaeota* (5.7 ± 0.71c) Firmicutes (37.53 ± 3.75b) Thermotogae (39.56 ± 4.46a)	Proteobacteria (2.75 ± 0.33c) Firmicutes (20.5 ± 0.87b) Thermotogae (65.23 ± 1.83a)
Flagellar assembly [PATH:ko02040]	Synergistetes (1 ± 0.29c) Spirochaetes (43.9 ± 2.46b) Firmicutes (52.28 ± 2.22a)	Synergistetes (0.78 ± 0.2c) Spirochaetes (34.02 ± 3.67b) Firmicutes (62.68 ± 3.27a)	Proteobacteria (2.89 ± 1.03c) Thermotogae (23.85 ± 7b) Firmicutes (66.84 ± 5.14a)	Proteobacteria (2.39 ± 0.9b) Firmicutes (45.34 ± 6.4a) Thermotogae (48.85 ± 7.57a)
Oxidative phosphorylation [PATH:ko00190]	Spirochaetes (8.5 ± 0.21c) Euryarchaeota (26.4 ± 3.66b) Firmicutes (36.23 ± 2.36a)	Spirochaetes (8.94 ± 2.06c) Firmicutes (20.44 ± 0.81b) Euryarchaeota (45.85 ± 5.64a)	Thermotogae (4.28 ± 0.51c) Firmicutes (21.31 ± 1.53b) Euryarchaeota* (68.91 ± 1.24a)	Thermotogae (19.73 ± 3.19c) Firmicutes (31.08 ± 0.28b) Euryarchaeota (40.16 ± 4.47a)
Methane metabolism [PATH:ko00680]	Euryarchaeota	Euryarchaeota	Euryarchaeota	Euryarchaeota

The top three contributors in each pathway are shown.
* The proportion positively correlate with DCP ($p < 0.01$). The values in the brackets indicate the contributive proportion in the relative abundance of these pathways. Values in a column with different letters mean significant differences at $p < 0.05$. All data are presented as means ± standard deviations.

(Lie et al., 2012). Thus, if the proton gradient cannot be immediately used for ATP synthesis through oxidative phosphorylation, the accumulative proton gradient will hinder the electron transport due to feedback inhibition and probably hurt the cytomembrane due to overload of potential difference. The contributive proportions of Euryarchaeota in the relative abundance of oxidative phosphorylation increased with temperature from 25 °C (26%) to 50 °C (69%), further implying that oxidative phosphorylation had tight relationship with methanogenesis and probably played crucial role in methane production at 50 °C. The flagellar assembly, indicating the cellular motility (Cui et al., 2013; Zhang et al., 2014), positively correlated with temperature ($p < 0.01$), implying that more microorganisms especially in the phylum Firmicutes actively tended to access substrates at thermophilic condition (Zhang et al., 2014).

The ABC transporters comprise one of the largest protein families, and are also involved in a wide variety of physiological functions, such as antibiotic resistance and uptake of various nutrients (Higgins, 2001).They also positively correlated with temperature ($p < 0.01$). Interestingly, only at 50 °C, the phylum mainly involved in ABC transporters included Euryarchaeota, and this implied that the uptake of various nutrients for methanogens was strengthened at 50 °C. In addition, the proportions of Euryarchaeota involved in each of these pathways (except flagellar assembly) increased with temperature from 25 to 50 °C and showed positive correlation with DCP ($p < 0.01$), indicating that more proportions of these pathways were directly served for methane production at 50 °C. The lower relative abundances of oxidative phosphorylation and methanogenesis, and lower proportions of Euryarchaeota participating in these core pathways at 55 °C than 50 °C, further explained reduced methane production at 55 °C.

Consequently, these data suggested that temperature regulated the methane production probably through strengthening these pathways especial for oxidative phosphorylation and methanogenesis.

3.5. Function diversity and centralization

Whether the diversity of functional pathways at level 3 correlated tightly with efficiency, redundancy and stability of system functioning (mainly referred to methane production) was also explored in this study. The alpha-diversity indices, including Shannon index, Simpson index and Pielous' evenness of functional pathways, showed a linear and negative correlation with DCP (Fig. 3). The alpha-diversity indices decreased with temperature from 25 to 50 °C, and rebounded at 55 °C (Table 3). The centralization of functional pathways (function centralization) was assessed by the least proportion of functional pathways contributing for at least 50% of total reads at level 3. Low proportion indicated high

Table 3
The alpha-diversity of functional pathways at level 3, annotated based on the KEGG Orthologs datasets at different temperatures.

	25 °C	35 °C	50 °C	55 °C	DCP	Temperature	Acetate	Propionate	Butyrate
Shannon index	3.682 ± 0.044b	3.538 ± 0.007b	3.194 ± 0.076a	3.329 ± 0.02a	−.853**	−.870**	.779**	.876**	.745**
Simpson index	0.956 ± 0.004c	0.944 ± 0.001bc	0.902 ± 0.015a	0.928 ± 0.001b	−.832**	−.709**	.653*	.722**	.609*
Pielou's evenness	0.72 ± 0.01c	0.695 ± 0.001bc	0.639 ± 0.013a	0.677 ± 0.003b	−.886**	−.756**	.757**	.782**	.703*
Gini coefficient	0.542 ± 0.003b	0.547 ± 0.001b	0.555 ± 0a	0.544 ± 0.003b	.828**	.375	−.513	−.368	−.496

All data are presented as means ± standard deviations. Values in a row with different letters mean significant differences at $p < 0.05$. **Significantly at $p < 0.01$; *$p < 0.05$.

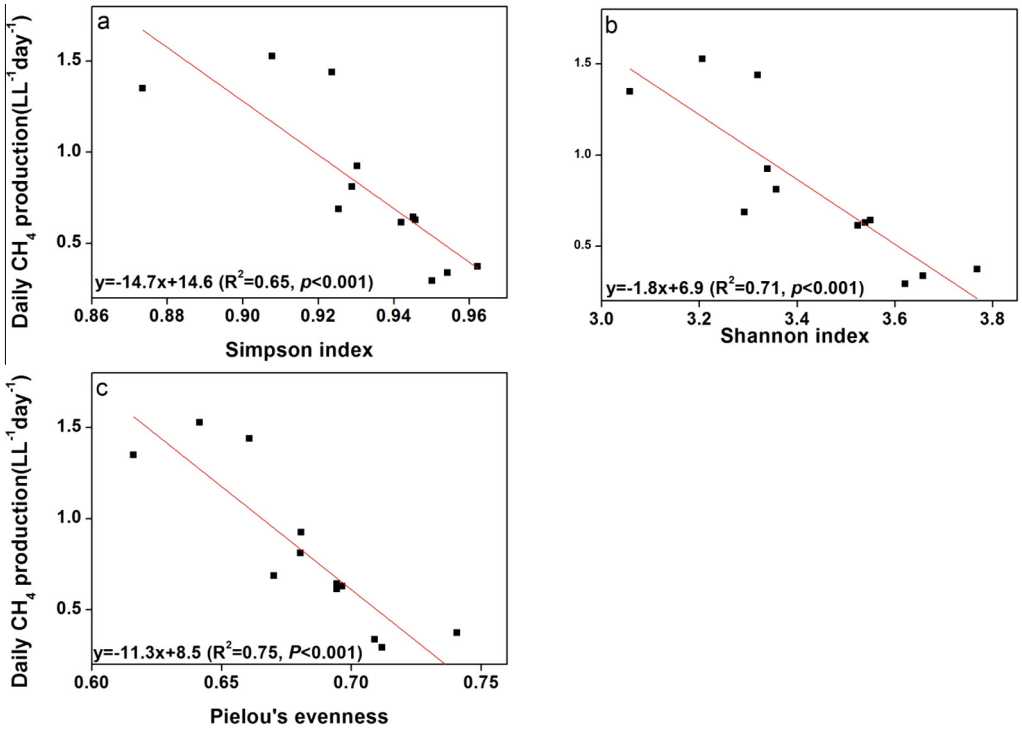

Fig. 3. The relationship between the different alpha-diversity parameters (a) Simpon index, (b) Shannon index and (c) Pielous' evenness of functional pathways at level 3 and daily methane production.

function centralization. Overall, at each temperature, the high function centralization could be observed, since around 50% of total reads focused on 5.6 ± 0.3, 4.9 ± 0.4, 3.6 ± 0.2 and 4.8 ± 0.3% of functional pathways at 25, 35, 50 and 55 °C, respectively (Supplementary Fig. S8a). Especially at 50 °C, the highest function centralization occurred, as around 50% of total reads was concentrated mainly on 5 function categories, occupying around 3.6% of total function categories. These functional pathways were methane metabolism (26%), ABC transporters (9.9%), flagellar assembly (8.1%), oxidative phosphorylation (5.8%) and ribosome (5.3%) (Supplementary Table S3). The function centralization also showed a clear positive linear correlation with DCP ($p < 0.01$) (Supplementary Fig. S8b). The Gini coefficient, widely used as an index of evenness (Werner et al., 2011; Wittebolle et al., 2009), was introduced to reflect the function centralization. The high Gini coefficient indicated high centralization in this study (Table 3). The Gini coefficient increased with temperature from 25 to 50 °C, but decreased at 55 °C, and showed a clear linear positive correlation with DCP (Supplementary Fig. S9).

A high alpha-diversity of the microbial community provides high system stability (Naeem and Li, 1997; Werner et al., 2011). Most studies concerning the evaluation of biodiversity focus on microbial community composition (Ma et al., 2015; Maestre et al., 2015), and rarely on functional pathways, which might be more essentially related to the activities of important functions, such as methane production. In this study, the alpha-diversity of functional pathways showed a negative correlation with methane production ($p < 0.01$), which was opposite to the relationship between alpha-diversity of microbial community composition and methane production (Werner et al., 2011). A high alpha-diversity of microbial community, determined by the microbial species quantity and distribution, corresponds with functional redundancy, based on the overlap and complementarity of the microbial functional potential (Werner et al., 2011). However, the alpha-diversity of functional pathways based on Metatranscriptomic analysis can be considered a more essential evaluation of the diversity of microbial functions, and a more actual reflection of system functioning. The diversity of microbial community can be considered a mere description of the different microorganisms that have various functional potentials in a certain environment, while the diversity of functional pathways describes which processes these microorganisms are actively involved in. Hence, due to the overlap of microbial function and/or the versatility of some specific microorganisms (Vanwonterghem et al., 2014), the diversities based on microbial community composition and functional pathways, may show an inconsistent response to specific system functioning, such as methane production.

In this study, a low diversity of functional pathways indicated high function centralization. Overall, high function centralization was observed at all temperatures, which might be related to anaerobic digestion metabolism. This study showed that only the relative abundance of methanogenesis was higher than 10% of total reads at each temperature (Supplementary Table S3), indicating that metabolic activity related to methane production must play a crucial role in the high function centralization. The function centralization was linearly correlated with methane production under the temperature gradient. Based on these functional pathways which were used to evaluate the centralization at different temperatures, the accumulative relative abundances contributed by Euryarchaeota accounted for 13% at 25 °C, 16% at 35 °C, 32% at 50 °C and 14% at 55 °C in total reads (Supplementary Table S3), and they positively correlated with DCP. This demonstrated that methanogens played crucial role in the high function centralization.

In general, the expression of functional pathways in microbial community is regulated by environmental factors, such as temperature (Vanwonterghem et al., 2014). In this study, although the high centralization of functional pathways in thermophilic AD process might be caused by the inhibition of some pathways due to high temperature or temperature-induced toxic compounds, this did reflect the life strategies of microbial community responding to different temperatures. Because methane production process needs harmonious expressions of various functional pathways conducted by fermentative bacteria and methanogenic archaea, simply and randomly reduction of functional pathways would probably result in the collapse of AD process. Thus, it reasonably indicated that the life strategies of microbial community influenced by temperature essentially induced the difference of system functioning. In consideration of different life strategies of microbial community at different temperatures, the function centralization varied with temperatures, indicating that the activity of the microbial community in the AD system was differentially allocated to different pathways. High function centralization indicates that more cellular activities focus on fewer functional pathways. In complex but functionally enriched systems, different expression abundances of specific functional pathways dependent on cellular activities will determine the activities of substrate biodegradation pathways and therefore, also the final products of the process (Vanwonterghem et al., 2014). If the cellular activities of the microbial community mainly focus on specific functional pathways, these functions will be strengthened. On the contrary, if the cellular activities of the microbial community are evenly allocated to several different functional pathways, the system may be highly versatile. Thus, fine trade-off of different functions in a system with multifunctionality probably does not induce high efficiency of each function. In AD systems, high methane production rates are to be targeted. Due to existence of extensive conversion pathways of organic waste, an even expression of functional pathways may result in various intermediates and final metabolites, including not only CH_4 and CO_2, but also other compounds (Weiland, 2010). This could be regarded as "wasting" of resources, thus, an oriented and efficient conversion of the organic waste to methane is preferred. Overall, a high CH_4 content in the biogas, corresponding with high function centralization, indicated that high function centralization restrained alternative conversion pathways of untargeted final metabolites. This effectively reduced the "waste" of resources.

Consequently, first, a high function centralization strengthened specific fermentative functions, especial for methanogenesis, which was particularly highlighted at 50 °C where methanogenesis, occupying 26% of total reads, contributed most to the high function centralization. In addition, high expression of ABC transporters, flagellar assembly and oxidative phosphorylation both directly and indirectly improved methanogenesis. Hence, the majority of cellular activities were invested in methanogenesis and related pathways to strengthen methane production. The increasing accumulative relative abundances from Euryarchaeota with temperature from 25 to 50 °C implied that more methanogens participated in these pathways, which further supported the viewpoint above. The proportion of Euryarchaeota involved in each of these pathways (except flagellar assembly) increased with temperature from 25 to 50 °C and showed positive correlation with DCP ($p < 0.01$), indicating that in each of these pathways, more chances and resources were attained by methanogens as temperature increased. This probably resulted in high methane production at 50 °C and also supported viewpoint of function centralization concerning methane production. Second, a high centralization of functional pathways oriented the extensive conversion of substrates into desirable products, such as methane. A high centralization of functional pathways enhancing the efficiency of substrates conversion into methane was partly supported by total biogas production, which representing the accumulative conversion of substrates to biogas, and showing a similar changing trend as the

centralization of functional pathways at different temperatures. High proportions of functional pathways conducted by Euryarchaeota which primarily performed the methanogenesis further supported the second viewpoint. Although the viewpoint of function centralization concerning functional efficiency needs more data to verify, e.g. comparison between different substrates, a brand-new viewpoint is supplied to further evaluate the relationship between biodiversity and system functioning.

4. Conclusions

Metatranscriptomic analysis revealed the relationship between the variations of functional pathways and methane production in AD systems at different temperatures. In contrast to the fact that a high microbial community diversity increased redundancy of the functional potential, a low diversity of functional pathways was found to strengthen specific functions, especial for methanogenesis, and enhance the efficiency of oriented conversion of substrates into methane. Consequently, one of temperature-regulated mechanisms on methane production was probably realized through centralization of functional pathways by reducing the diversity of functional pathways, but enhancing central functional pathways in AD systems.

Abbreviations

AD: Anaerobic digestion; VFAs: Volatile fatty acids; DCP: Daily CH_4 production ($L\ L^{-1}day^{-1}$); PCoA: Principal coordinates analysis; RDA: Redundancy analysis; PERMANOVA: Permutational multivariate analysis of variance; HRT: Hydraulic retention time; OLR: Organic loading rate; VS: Volatile solid; TS: Total solid; COD: Chemical oxygen demand; ANOVA: One-way-analysis of variance; KO: KEGG Orthologs; EC: Enzyme commission; ABC transporters: ATP-binding cassette transporters.

Competing interest

All authors declare that they have no competing interests.

Authors' contributions

QL performed the experimental work, data analysis and writing. JDV was involved in the improvement of paper. GH was involved in the experimental work. JL, XL was involved in the experimental design and improvement of paper. All authors read and approved the final manuscript.

Acknowledgements

This work is supported by 973 project (No. 2013CB733502), National Key Technology Support Program (2014BAD02B04) and Open Found of Key Laboratory of Environmental and Applied Microbiology CAS (KLCAS-2016-03). Jo De Vrieze is supported as a postdoctoral fellow from the Research Foundation Flanders (FWO- Vlaanderen).

Appendix A. Supplementary data

Supplementary data associated with this article can be found, in the online version, at http://dx.doi.org/10.1016/j.biortech.2016.05.046.

References

APHA, 1998. Standard Methods for the Examination of Water and Wastewater. American Public Health Association, Washington, DC.
Bludman, S.A., Vanriper, K.A., 1977. Equation of state of an ideal ferni gas. Astrophys. J. 212 (3), 859–872.
Cui, W.R., Chen, L., Huang, T., Gao, Q., Jiang, M., Zhang, N., Zheng, L.L., Feng, K.Y., Cai, Y.D., Wang, H.W., 2013. Computationally identifying virulence factors based on KEGG pathways. Mol. BioSyst. 9 (6), 1447–1452.
de Menezes, A., Clipson, N., Doyle, E., 2012. Comparative metatranscriptomic reveals widespread community responses during phenanthrene degradation in soil. Environ. Microbiol. 14 (9), 2577–2588.
De Vrieze, J., Verstraete, W., Boon, N., 2013. Repeated pulse feeding induces functional stability in anaerobic digestion. Microb. Biotechnol. 6 (4), 414–424.
De Vrieze, J., Saunders, A.M., He, Y., Fang, J., Nielsen, P.H., Verstraete, W., Boon, N., 2015. Ammonia and temperature determine potential clustering in the anaerobic digestion microbiome. Water Res. 75, 312–323.
Fredriksson, N.J., Hermansson, M., Wilen, B.-M., 2012. Diversity and dynamics of Archaea in an activated sludge wastewater treatment plant. BMC Microbiol. 12.
Gannoun, H., Omri, I., Chouari, R., Khelifi, E., Keskes, S., Godon, J.J., Hamdi, M., Sghir, A., Bouallagui, H., 2016. Microbial community structure associated with the high loading anaerobic codigestion of olive mill and abattoir wastewaters. Bioresour. Technol. 201, 337–346.
Gifford, S.M., Sharma, S., Booth, M., Moran, M.A., 2013. Expression patterns reveal niche diversification in a marine microbial assemblage. ISME J. 7 (2), 281–298.
Gifford, S.M., Sharma, S., Moran, M.A., 2014. Linking activity and function to ecosystem dynamics in a coastal bacterioplankton community. Front. Microbiol. 5.
Gunnigle, E., Nielsen, J.L., Fuszard, M., Botting, C.H., Sheahan, J., O'Flaherty, V., Abram, F., 2015. Functional responses and adaptation of mesophilic microbial communities to psychrophilic anaerobic digestion. FEMS Microbiol. Ecol. 91 (12).
Hart, S.C., Stark, J.M., Davidson, E.A., Firestone, M.K., 1994. Nitrogen Mineralization, Immobilization, and Nitrification. Methods of Soil Analysis: Part 2-Microbiological and Biochemical Properties (methodsofsoilan2), pp. 985–1018.
Higgins, C.F., 2001. ABC transporters: physiology, structure and mechanism – an overview. Res. Microbiol. 152 (3–4), 205–210.
Labatut, R.A., Angenent, L.T., Scott, N.R., 2014. Conventional mesophilic vs. thermophilic anaerobic digestion: a trade-off between performance and stability? Water Res. 53, 249–258.
Li, X.K., Ma, K.L., Meng, L.W., Zhang, J., Wang, K., 2014. Performance and microbial community profiles in an anaerobic reactor treating with simulated PTA wastewater: from mesophilic to thermophilic temperature. Water Res. 61, 57–66.
Lie, T.J., Costa, K.C., Lupa, B., Korpole, S., Whitman, W.B., Leigh, J.A., 2012. Essential anaplerotic role for the energy-converting hydrogenase Eha in hydrogenotrophic methanogenesis. Proc. Natl. Acad. Sci. U.S.A. 109 (38), 15473–15478.
Ma, Q., Qu, Y.Y., Zhang, X.W., Liu, Z.Y., Li, H.J., Zhang, Z.J., Wang, J.W., Shen, W.L., Zhou, J.T., 2015. Systematic investigation and microbial community profile of indole degradation processes in two aerobic activated sludge systems. Sci. Rep. 5, 11.
Maestre, F.T., Delgado-Baquerizo, M., Jeffries, T.C., Eldridge, D.J., Ochoa, V., Gozalo, B., Quero, J.L., Garcia-Gomez, M., Gallardo, A., Ulrich, W., Bowker, M.A., Arredondo, T., Barraza-Zepeda, C., Bran, D., Florentino, A., Gaitan, J., Gutierrez, J.R., Huber-Sannwald, E., Jankju, M., Mau, R.L., Miriti, M., Naseri, K., Ospina, A., Stavi, I., Wang, D.L., Woods, N.N., Yuan, X., Zaady, E., Singh, B.K., 2015. Increasing aridity reduces soil microbial diversity and abundance in global drylands. Proc. Natl. Acad. Sci. U.S.A. 112 (51), 15684–15689.
Marzorati, M., Wittebolle, L., Boon, N., Daffonchio, D., Verstraete, W., 2008. How to get more out of molecular fingerprints: practical tools for microbial ecology. Environ. Microbiol. 10 (6), 1571–1581.
Meyer, F., Paarmann, D., D'Souza, M., Olson, R., Glass, E., Kubal, M., Paczian, T., Rodriguez, A., Stevens, R., Wilke, A., Wilkening, J., Edwards, R., 2008. The metagenomics RAST server – a public resource for the automatic phylogenetic and functional analysis of metagenomes. BMC Bioinformatics 9 (1), 1–8.
Millares, L., Perez-Brocal, V., Ferrari, R., Gallego, M., Pomares, X., Garcia-Nunez, M., Monton, C., Capilla, S., Monso, E., Moya, A., 2015. Functional metagenomics of the bronchial microbiome in COPD. PLoS ONE 10 (12), 13.
Naeem, S., Li, S.B., 1997. Biodiversity enhances ecosystem reliability. Nature 390 (6659), 507–509.
Pap, B., Gyoerkei, A., Boboescu, I.Z., Nagy, I.K., Biro, T., Kondorosi, E., Maroti, G., 2015. Temperature-dependent transformation of biogas-producing microbial communities points to the increased importance of hydrogenotrophic methanogenesis under thermophilic operation. Bioresour. Technol. 177, 375–380.
Shi, W.B., Moon, C.D., Leahy, S.C., Kang, D.W., Froula, J., Kittelmann, S., Fan, C., Deutsch, S., Gagic, D., Seedorf, H., Kelly, W.J., Atua, R., Sang, C., Soni, P., Li, D., Pinares-Patino, C.S., McEwan, J.C., Janssen, P.H., Chen, F., Visel, A., Wang, Z., Attwood, G.T., Rubin, E.M., 2014. Methane yield phenotypes linked to differential gene expression in the sheep rumen microbiome. Genome Res. 24 (9), 1517–1525.
Sun, W.M., Yu, G.W., Louie, T., Liu, T., Zhu, C.S., Xue, G., Gao, P., 2015. From mesophilic to thermophilic digestion: the transitions of anaerobic bacterial, archaeal, and fungal community structures in sludge and manure samples. Appl. Microbiol. Biotechnol. 99 (23), 10271–10282.

Tian, Z., Zhang, Y., Li, Y.Y., Chi, Y.Z., Yang, M., 2015. Rapid establishment of thermophilic anaerobic microbial community during the one-step startup of thermophilic anaerobic digestion from a mesophilic digester. Water Res. 69, 9–19.
Vanwonterghem, I., Jensen, P.D., Ho, D.P., Batstone, D.J., Tyson, G.W., 2014. Linking microbial community structure, interactions and function in anaerobic digesters using new molecular techniques. Curr. Opin. Biotechnol. 27, 55–64.
Weiland, P., 2010. Biogas production: current state and perspectives. Appl. Microbiol. Biotechnol. 85 (4), 849–860.
Werner, J.J., Knights, D., Garcia, M.L., Scalfone, N.B., Smith, S., Yarasheski, K., Cummings, T.A., Beers, A.R., Knight, R., Angenent, L.T., 2011. Bacterial community structures are unique and resilient in full-scale bioenergy systems. Proc. Natl. Acad. Sci. U.S.A. 108 (10), 4158–4163.
Wilson, C.A., Murthy, S.M., Fang, Y., Novak, J.T., 2008. The effect of temperature on the performance and stability of thermophilic anaerobic digestion. Water Sci. Technol. 57 (2), 297–304.
Wittebolle, L., Marzorati, M., Clement, L., Balloi, A., Daffonchio, D., Heylen, K., De Vos, P., Verstraete, W., Boon, N., 2009. Initial community evenness favours functionality under selective stress. Nature 458 (7238), 623–626.
Yu, K., Zhang, T., 2012. Metagenomic and metatranscriptomic analysis of microbial community structure and gene expression of activated sludge. PLoS ONE 7 (5).
Zhang, H.S., Chen, X., Braithwaite, D., He, Z., 2014. Phylogenetic and metagenomic analyses of substrate-dependent bacterial temporal dynamics in microbial fuel cells. PLoS ONE 9 (9), 8.